Published in final edited form as:
Calcif Tissue Int. 2013 April ; 92(4): 372–384. doi:10.1007/s00223-012-9688-0.

The Influence of Therapeutic Radiation on the Patterns of Bone Remodeling in Ovary-Intact and Ovariectomized Mice

Susanta K Hui, Ph.D.[1,2], **Gregory R Fairchild, Ph.D.**[1,3], **Louis S Kidder, Ph.D.**[1], **Manju Sharma, Ph.D.**[1], **Maryka Bhattacharya, Ph.D.**[4], **Scott Jackson, M.S.**[5], **Chap Le, Ph.D.**[6], **Anna Petryk, Ph.D.**[7,8], **Mohammad Saiful Islam**[9], and **Douglas Yee, M.D.**[2,10]

[1]Department of Therapeutic Radiology, University of Minnesota, Minneapolis, MN, USA

[2]Masonic Cancer Center, University of Minnesota, Minneapolis, MN, USA

[3]United States Navy, Medical Service Corps, Minneapolis, MN, USA

[4]Departments of Medicine and Orthopaedic Surgery, Medical College of Georgia, Augusta, GA, USA

[5]Biostatistics and Informatics shared resource of Masonic Cancer Center, Minneapolis, MN, USA

[6]Department of Biostatistics, University of Minnesota, Minneapolis, MN, USA

[7]Department of Pediatrics, University of Minnesota, Minneapolis, MN, USA

[8]Department of Genetics, Cell Biology and Development, University of Minnesota, Minneapolis, MN, USA

[9]Department of Diagnostic and Biological Sciences, Masonic Cancer Center, University of Minnesota, Minneapolis, MN, USA

[10]Department of Medicine, Masonic Cancer Center, University of Minnesota, Minneapolis, MN, USA

Abstract

Purpose—To characterize changes in bone remodeling associated with localized radiation that models therapeutic cancer treatment in ovary-intact and ovariectomized mice and evaluate the influence of radiation on the pattern of bone mineral remodeling.

Methods—Young adult, female BALB/c mice, ovary-intact (I) and ovariectomized (OVX), were used (n=71). All mice were intravenously injection with 15 μCi ^{45}Ca. Thirty days post-^{45}Ca administration, the hind limbs of 17 mice were exposed to a single 16 Gy radiation (R). The time course of ^{45}Ca excretion, serum CTx and osteocalcin markers, and cancellous bone volume fraction (BV/TV) and cortical thickness (Ct.Th) of the distal femur were measured. Cellular activity and dynamic histomorphometry were performed.

Results—Irradiation resulted in rapid increases in fecal ^{45}Ca excretion compared to control groups, indicating increased bone remodeling. CTX increased rapidly after irradiation, followed by an increase in osteocalcin concentration. BV/TV decreased in the ovary-intact mice following

Address for correspondence: Susanta K Hui, Department of Therapeutic Radiology, University of Minnesota, 420 Delaware Street SE, Mayo Mail Code 494, Minneapolis, MN 55455, Phone: 612-626-4484, Fax: 612-626-7060; huixx019@umn.edu.

The authors have stated that they have no conflict of interest.

DISCLOSURES: All authors state that they have no conflicts of interest. The authors also state that they have full control of all primary data and they agree to allow *Calcified Tissue* to review their data if requested.

irradiation. Ct.Th increased in the OVX groups following irradiation. I+R exhibited diminished osteoblasts surface, osteoclast number and mineral apposition rate.

Conclusions—Our murine model showed the systemic effects (via ^{45}Ca excretion) and local effects (via bone microarchitecture and surface activity) of clinically-relevant, therapeutic radiation exposure. Ovary-intact and ovariectomized murine models have similar ^{45}Ca excretion but different bone microarchitecture responses. ^{45}Ca assay effectively indicates the onset and rate of systemic bone mineral remodeling, providing real time assessment of changes in bone histomorphometric parameters. Monitoring bone health via a bone mineral marker may help identify the appropriate time for clinical intervention to preserve skeletal integrity.

Keywords

clinically relevant radiation; biodistribution; bone remodeling; ^{45}Ca; ^{41}Ca surrogate

INTRODUCTION

Cancer survivors are a distinct population who may experience accelerated bone loss [1] over that of age-related osteoporosis. Women who undergo cancer therapy experience a 10–20% increased fracture risk from treatment-induced bone loss compared to healthy women [2, 3]. While decreased bone mineral density is associated with increased risk of fracture, recent work has demonstrated that remodeling status may be as predictive [4–9]. Significantly, Riggs et al. found that high bone turnover substantially contributes to vertebral fracture risk because of its disruptive effect on the micro-architecture of cancellous bone [9]. Furthermore, a recent study shows that recovery from radiation induced skeletal damage following anti-resorptive therapy may depend on ovarian function (i.e., pre- and post-menopausal status) [10]. Thus, insight into the extent and nature of post treatment skeletal damage is also essential to determine the optimal preventive treatment management.

Some of the factors that adversely influence bone mineral remodeling in female cancer patients are inherent to current cancer treatment regimens. Premenopausal patients with pelvic-area cancers routinely undergo ovariectomy to induce an acute estrogen deficiency to improve treatment success of estrogen-sensitive cancers. These patients are at an increased risk of osteoporosis. Patients are also at increased risk of bone fractures due to the adverse effects of the treatment itself (radiation and/or chemotherapy) [3, 11]. Thus, skeletal homeostasis of many patients with pelvic-area cancers is impacted by both acute estrogen deficiency and therapeutic doses of radiation.

Biochemical markers of bone turnover correlate to bone formation and resorption events and are measurable in blood or urine (4,5). They respond rapidly to treatments or other perturbations of bone turnover and can be assessed repeatedly in human subjects to track changes over time. However, a lack of specificity and high variability limits their utility in the clinical setting. Furthermore, while markers reflect changes in bone, they do not allow quantification of absolute changes expressed in bone units; only relative changes in the formation or resorption via collagen degradation process are reported.

With bone being composed of ~70% mineral [12] and calcium representing nearly half of all bone mineral, calcium tracers offer a logical, noninvasive approach to measuring changes in bone turnover. Additionally, the ability to develop a kinetic model will assist insight into the in- and out- flow of bone calcium during skeletal homeostasis and following systemic perbutations such as endocrine disruption and irradiation (e.g., see Weaver group [13] and Hui group [14]. Kinetic modeling will aid in understanding the nature of calcium flow rates (rapid, slow or mixed), thus potentially addressing possible mechanisms for alterations in skeletal physiology affected by radiation. Implementation of a calcium tracer may allow

early as well as longitudinal monitoring of bone responses to clinical therapies. Monitoring remodeling over time may be of value because alterations in bone remodeling precede changes in bone mineral density [15–17].

Assaying the excretion of a calcium isotope (such as ^{41}Ca or ^{45}Ca) over time may provide a useful tool to non-invasively monitor changes in bone turnover. The utility of this approach has recently been demonstrated by quantifying bone turnover in response to bisphosphonate treatment [18]. The skeletal uptake of a calcium isotope (e.g., ^{41}Ca which can be delivered in ~nanocurie quantities) is compared with elution via excreta, quantified by accelerator mass spectrometry for ^{41}Ca, or using commonly available liquid scintillation counting systems for ^{45}Ca [18, 19]. These radioisotopes of calcium behave identically to dietary calcium *in vivo*; both ^{41}Ca and ^{45}Ca are already established as tracers used for calcium metabolism studies [20]. ^{45}Ca is a preferred marker in non-human animal models because of its short half-life (164 days), ease of measurement and minimal expense. By quantifying the pharmacokinetics of this isotope in an animal subjected to irradiation and/or acute estrogen deficiency, this investigation aims to provide a basis for the clinical use of ^{41}Ca to non-invasively monitor bone turnover in human. ^{45}Ca has been shown to be useful as a marker reflecting bone turnover as validated by the Weaver group in a non-irradiated OVX rat [13]. The currently discussed work examines the effect of localized radiation on intact and OVX rodent models.

Overall, our purpose was to: A) Validate a murine model to characterize the varying degrees of bone loss associated with therapeutic cancer treatments used to treat post-menopausal women (i.e. clinically relevant radiation dose in animals with acute estrogen-deficiency). A targeted and biologically equivalent dose of radiation to the appendicular skeleton is used in this investigation as a model of radiation therapy, for example, for treating endometrial cancer; and, B) Evaluate the influence of clinically relevant, therapeutic radiation on patterns of bone remodeling in ovary-intact and ovariectomized murine models, correlating changes in bone surface activity and microarchitecture with bone mineral turnover as measured via ^{45}Ca excretion.

METHODS

Five groups of skeletally mature BALB/c female mice (16 weeks old) were used for this study. The schematic representation of the design of this study is shown in Figure 1. Both ovary-intact (I) and ovariectomized (OVX) mice were chosen to mimic the clinical management of pre-menopausal and menopausal cancer patients undergoing radiation therapy (R), with appropriate controls. The examined groups were: 1) “BD” (biodistribution, n=20); 2) “I−R” (control, n=17); 3) “I+R” (irradiated, n=19); 4) “OVX−R” (control, n=7); and, 5) “OVX+R” (irradiated, n=8). The number of mice within the BD, I−R and I+R groups allowed for the sacrifice of mice at multiple time points. Additional animals were also added to the I+R and OVX+R groups to account for possible loss of mice due to possible complications associated with radiation exposure (i.e. weight loss, organ toxicity, etc.). Mice were ovariectomized by the vendor 57 days prior to irradiation (Jackson Laboratory; Bar Harbor, ME). This study was approved by the University of Minnesota Institutional Animal Care and Use Committee (IACUC).

Animal Husbandry

In order to monitor health, mice were weighed prior to irradiation and every day following irradiation for 10 days, as well as prior to placement in metabolic collection cages. Mice were housed 3–5 per cage, in a temperature- and humidity-controlled room with free access to a standard rodent diet containing 18.6% protein, 1% calcium, and 1.5 IU/g added vitamin D (2018; Harlan Teklad, Madison, WI) and water. Mice were acclimated to a 12-hour light/

dark cycle. A minimal decline in mean body weight (0.5 to 1gm) in the radiation group compared to non-irradiated group was observed as expected. This small difference in body weight (2–4%) is not expected to affect the results of our study.

^{45}Ca Delivery

After a week of acclimation in the vivarium, all mice were given an intravenous injection of 0.1 mL biostatic saline containing 15 μCi of $^{45}CaCl_2$. For the OVX±R groups, this injection was 27 days post ovariectomy (i.e., at skeletal homeostasis).

Estimation of clinically relevant radiation dose

Because a variety of fractionation schema have been used among clinical trials, Fowler (18) suggested using the normalized total dose (NTD), which is the biological effective dose (BED) normalized to a 2Gy fraction.

$$(\text{BED}=\text{total dose}\,(1+\text{d}/[\alpha/\beta]);\text{NTD}=\text{BED}/\text{RE in equivalent 2Gy fractions}) \quad (1)$$

d is the dose per fraction, the α/β is the ratio of intrinsic radiosensitivity to repair capability of a specified tissue [21]. The α/β is assumed to be 3 Gy for late normal-tissue complications. RE = (1+d/[α/β]) is the relative effectiveness for 2 Gy per fraction. The dose rate is assumed to have a negligible effect. In clinical practice, radiation dosage delivered to the pelvic region varies mostly within 40–60 Gy (2 Gy/fraction). For late normal-tissue complications, a physical dose of 60 Gy (2 Gy/fraction) is equivalent to a BED of 100 Gy and a NTD of 60 Gy. A single dose of 16 Gy is equivalent to a BED of 101.3 Gy and a NTD of 60.8 Gy; therefore, as a simplified murine model, a one-time exposure of 16 Gy can be used to accurately simulate clinical irradiation of bone tissue. Additionally, the irradiated skeletal portion in the murine model included both hind limbs, as described below. This area represented an average of approximately 20 percent of the total murine skeleton (as measured by posthumous dry bone weight) and is approximately equal to the percent of total skeleton in the average irradiated pelvic region (20–30% as measured by CT) of a clinical subject. The areas of comparison between our murine model and clinical subjects also have comparable amounts of total skeletal trabecular bone volume.

Radiation Delivery

All mice in the I+R and OVX+R groups were irradiated once ^{45}Ca reached a steady state of excretion (30 days after ^{45}Ca injection). A Philips RT250 orthovoltage unit operating at 250 kVp was used for all irradiations. The radiation output was calibrated according to guidelines set by the American Association of Physics in Medicine Task Group 61 calibration protocol for calibration of low-energy orthovoltage units [22, 23]. To facilitate radiation delivery, all mice in the I+R and OVX+R groups were anesthetized using a 0.05 mL intraperitoneal injection of a cocktail of ketamine (100mg/kg) and xylazine (10 mg/kg). All mice in the I−R and OVX−R groups were also anesthetized to control for the possible impact of anesthesia on bone metabolism. Once anesthetized, the I+R and OVX+R mice were placed on a warmed acrylic plate for radiation delivery. The mice were secured to the plate using tape to minimize possible movement during irradiation. A specially designed lead shield was placed over the body cranial to the femur, over the pelvis and caudal vertebrae, targeting the radiation exposure to only the hind limbs (Figure 2 A). The shield over the main body had an average minimum thickness of 4 mm. Proper placement of shielding was confirmed using Kodak EDR-2 film placed beneath the acrylic plate and approximately 60 cGy radiation exposure. Following shielding placement verification, mice were monitored during the entire irradiation to ensure each mouse remained still with the critical organs properly protected. A source-to-surface of the leg distance (SSD) of 30.4 cm

was used. Total dose delivered, including the shielding placement exposure, was 16 Gy. Total dose was verified using micro thermo-luminescent dosimeters (micro-TLD).

^{45}Ca assay

While histomorphometric parameters are a cumulative measurement of changes over time, the kinetics of skeletal mineral remodeling can be measured by changes in excretion of ^{45}Ca. Details of ^{45}Ca measurement in excreta (e.g. feces and urine) by liquid scintillation was recently published by Hui et al.[24]. Briefly, feces and urine were collected for 24 hours in metabolic cages approximately every 3 days for up to 60 days following ^{45}Ca administration. Feces were oven dried at 80° C for 24 hours, homogenized through grinding, then weighed. Results were standardized by using 0.2 gm feces from each dried sample for digestion into solution for liquid scintillation counting. This solution was attained by dissolving the feces fraction into 2 mL of concentrated (37%) nitric acid. Twenty-four hours later, 1ml of hydrogen peroxide was added to decolorize the solution. Another 24 hours later, 0.4 mL of 3M HCl and 0.8 mL of deionized water were added to the solution. After a third and final 24 hour period in the digestion process, a 0.5 mL aliquot of the feces solution was combined with 15 mL of Ecolite scintillation cocktail for ^{45}Ca isotope counting. Urine was collected directly from the cage bottom by using 18 mL warm deionized water to rehydrate dried urine into solution. Results were standardized by concentrating 10 mL of the collected urine solution for liquid scintillation counting. The measured urine was concentrated by maintaining the sample at 80° C until completely dehydrated (24–48 hours), then rehydrating it using 1 mL of warm deionized water. Once concentrated, 15 mL of Ecolite scintillation cocktail was immediately added to the urine sample for counting. ^{45}Ca radioactivity in the excreta was measured in disintegrations per minute (DPM) during a 6 minute count by liquid scintillation (Beckman Coulter LS 6500; Indianapolis, IN). Variances in DPM due to the radioactive decay of the calcium isotope over time were accounted for by decay correcting all results to the day of injection.

To examine the biodistribution of ^{45}Ca, 5 mice from the BD group were euthanized by CO_2 anoxia on each of days 1, 3, 5, and 16 after ^{45}Ca administration. After sacrifice, blood was immediately collected by cardiac puncture. Serum was obtained by centrifugation (5 minutes, 3000 rpm). Femur, tibia, lumbar vertebrae, liver, kidneys, gut tissue (duodenum to anus, with contents), and the quadriceps femoris muscle were removed, washed with isotonic saline solution and weighed. The tissue samples were ashed for 48 hours in a muffle furnace at 525° C, then dissolved into a solution of 1 ml of 3M HCl and 1 ml of deionized water. A 0.5ml aliquot of the digested organ sample was combined with 15 mL of Ecolite scintillation cocktail (MP Biomedicals; Solon, OH).

Time course

In order to examine the time course of the radiation effect on bone remodeling, mice from the I±R groups were euthanized by CO_2 anoxia at different time points after irradiation. Five mice from both the I–R and I+R groups were sacrificed on each of Days 3 and 8 post-radiation, with the remaining I–R (n=7) and I+R (n=9) mice being euthanized 30 days post-radiation. The OVX±R groups were euthanized only at 30 days after irradiation.

CTx and osteocalcin assay

After sacrifice, blood was immediately collected by cardiac puncture in order to measure C-terminal telopeptide (CTx), a metabolic product of Type 1 collagen destruction (i.e., a marker of bone resorption) and osteocalcin (i.e., a peptide associated with bone mineralization). These measurements were necessary to validate radioisotope-associated bone responses with established biochemical markers. Both of these systemic features were assayed by sandwich ELISA kits (Biomedical Technologies, Inc.; Stoughton, MA). The

CTX kit had a sensitivity of 1 ng/ml, intraassay variation of 6% (95% limits), and interassay variation of 8% (95% limits). The osteocalcin kit had a range of 1–50 ng/mL, a sensitivity of 0.4 ng/ml, intraassay variation of 4%, and interassay variation of 6%.

Ovariectomy verification

Wet uterine weights of mice from the I±R and OVX±R groups were measured immediately post-mortem to verify efficacy of vendor-performed ovariectomies. Ovary-intact mouse uterii weighed an average of 0.0614 g ± 0.0052 SEM, while the average for ovariectomized mice was 0.0137 g ± 0.0020 SEM. This reduction in uterine weight of nearly 80% ($p=<0.001$) confirms the complete excision of all ovarian tissue.

MicroCT and Histological Analyses

Bone microarchitecture of I±R and OVX±R mice was analyzed with a microCT Scanner (μCT 35, Cone-Beam microCT, Scanco Medical, Switzerland) using protocols described by Bouxsein et al. [25]. Immediately after sacrifice, femora (n=20) were placed in 70% ethanol. The distal femoral metaphysis was scanned within a region of 0.3–1.0 mm from the growth plate in order to avoid the primary spongiosa, with a slice thickness of 7 μm resolution (100 slices) at 70 kVp. Using the manufacturer's software, relative cancellous bone volume fraction (BV/TV; %; i.e. the ratio of the segmented bone volume to the total volume of the region of interest) and cortical thickness (Ct.Th; mm) were estimated. The specimens were then demineralized with 0.5M EDTA, embedded in paraffin following dehydration, sectioned at 5 um, and stained with hematoxylin and eosin. Sections were imaged at 100x and bone surface cellular activity quantified as percent total Trabecular Perimeter (Tb.P), surface occupied by osteoblasts (Ob.S) and the number of osteoclasts (Oc.N) (Figure 2B).

Dynamic Histomorphometry

In order to evaluate bone activity over time, some mice were serially injected with flurochromes to label active surfaces [26, 27] Twelve mice (same sex, and age as before) were irradiated in hind limb with 16Gy as described earlier. Twelve days later, all mice received 37.5 mg/Kg tetracycline i.v. This acts to systemically mark actively forming bone surfaces. Seventeen days later (29d post-radiation), all mice received 37.5 mg/Kg i.v. calcein. Mice were euthanized five days later (34d post-radiation), thereby allowing for full incorporation of the fluorochrome. Tibiae were dissected out, soft tissues removed, and bone was fixed in 10% buffered formalin for 24 hours. Specimens were then transferred to cold 70% ethanol until they were vacuum embedded in methylmethacrylate. These blocks were sectioned at 5 um in the coronal plane and processed by EXAKT system (EXAKT Technologies, Inc.; Oklahoma City, OK). Bone sections were imaged under UV light (D350/50 excitation; D460/50 emission) on a Zeiss AxioPlan II (Oberkochen, Germany) equipped with an OASIS Glide S2 motorized XY stage from Objective Imaging (Cambridge, UK). Sections were captured with a 40x objective and stitched into a single high resolution image by Image-Pro v7.0 with the Stage-Pro module (Media Cybernetics, Inc., Rockville, MD) as shown in Figure 2C. Distance between flurochrome labels and label lengths were measured with ImageJ software.

Statistical Analysis

^{45}Ca excretion results were analyzed using a linear mixed model in SAS ver. 9.2 (Cary, NC) due to the presence of repeated measures. For comparisons of radiation vs. non-radiation mice within specific group-cohorts (I±R and OVX±R), we fit main effects for radiation and day as well as an interaction term. For comparisons of mice with matching radiation treatments between group-cohorts, a similar model was used but with group-cohort as an

effect instead of radiation. We calculated differences with relation to the outcome of ^{45}Ca as well as differences in rate of change (slope) of ^{45}Ca excretion over time.

CTx and osteocalcin were compared between radiation and non-radiation mice within each group-cohort by the use of two-sample t-tests.

Histomorphometric data were compared between radiation and non-radiation mice within each group-cohort by two-sample t-tests. Comparisons were also made between specific group-cohorts for both radiated and non-radiated mice. For the I±R groups, a generalized linear model was utilized due to the presence of three time points. Both histomorphometric outcomes were compared between each pair of time points after using a Tukey-Kramer adjustment for multiple comparisons. A correlation between cumulative ^{45}Ca and BV/TV for the I+R group was also calculated using the Pearson correlation coefficient.

Lastly we compared mice with the same radiation treatment in the I±R groups between days 3, 8 and 30 for cumulative ^{45}Ca excretion and BV/TV using a one-way Analysis of Variance (ANOVA).

RESULTS

Biodistribution and Pharmacokinetics of ^{45}Ca

Figure 3A shows that of the samples collected, gut tissue, spine and tibia exhibited the highest amounts of ^{45}Ca on Day 1 (mean ± SE, n=5) ($15.4 \pm 2.4 \times 10^4$ dpm, $15.2 \pm 1.2 \times 10^4$ dpm and $12.0 \pm 0.9 \times 10^4$ dpm, respectively) compared with other tissue sites. Skeletal muscle and serum had average ^{45}Ca contents on Day 1 of $9.3 \pm 3.3 \times 10^4$ dpm and $7.1 \pm 1.9 \times 10^4$ dpm, respectively, while liver and kidney retained far less ^{45}Ca ($0.50 \pm 0.04 \times 10^4$ dpm and $0.39 \pm 0.04 \times 10^4$ dpm, respectively). The amount of ^{45}Ca measured in the gut, serum, liver, and kidney decreased an average of 69.9% ± 4.5% from Day 1 to Day 3. The amount of ^{45}Ca in muscle decreased 93.0% during the same time period. By Day 16, the amount of ^{45}Ca in those specimens had decreased by an average of 96% ± 1.8%. The spinal ^{45}Ca concentration fluctuated over time, but had an average increase of 15.1% from the amount on Day 1. Tibial ^{45}Ca also remained high, within an average change of 3.8% compared to Day 1.

Figure 3B shows that ^{45}Ca excretion was greater in feces than urine. Feces contained an average 83.1% of all excreted ^{45}Ca. The total ^{45}Ca in feces and urine represented 26.1%, 8.2%, 3.1%, and 1.2% of the ^{45}Ca in the whole body on days 1, 3, 5, and 16, respectively. The sum of ^{45}Ca in feces and urine for Day 3 (22.4×10^4 dpm) is approximately equal to the total decrease in all soft tissues from Day 1 to Day 3 (25.4×10^4 dpm). An analogous observation applies to the ^{45}Ca measurements in excreta on Days 5 (8.00×10^4 dpm) and 16 (2.30×10^4 dpm) compared to the observed decreases in soft tissue from Days 3 to 5 (4.19×10^4 dpm) and Days 5 to 16 (2.20×10^4 dpm).

Four fold higher ^{45}Ca in feces compared with urine was observed in both pre- and post-radiation administration. A well-controlled diet likely contributed to the consistency of this ratio. All mice (I±R and OVX±R) reached a steady state of ^{45}Ca excretion around the same time; by approximately 25–30 days post ^{45}Ca injection (Figure 3C).

^{45}Ca excretion

The impact of radiation on bone mineral remodeling as measured by ^{45}Ca excretion was readily evident in all irradiated mice, with increased excretion indicating higher bone turnover (Table 1 and Figure 4). Notably, the onset of radiation effects was rapid in all irradiated mice, showing an increase of ^{45}Ca excretion by Day 4 post radiation compared to

the non-irradiated mice (Figure 4). Significant differences in ^{45}Ca were found between radiation and non-radiation mice within the I±R groups only (Estimate=−889.13, p<0.001), with the increased ^{45}Ca excretion indicating an increase in bone turnover in the I+R group compared to the I-R group. There were no significant differences in the rate of change over time within the four group-cohorts of interest. Complete results are shown in Table 2.

CTx and osteocalcin assay

To compare the results of ^{45}Ca as a bone mineral turnover marker with established bone biochemical markers, we measured serum concentrations of systemic markers of bone resorption (CTx) and formation (osteocalcin).

Significant differences in CTx measures were found among the ovary-intact group, with higher levels being observed in I+R mice compared to I-R mice on Day 3 (+38.2%, p=0.030). The same group also showed significant differences in osteocalcin level on Day 30, with higher levels being observed in I+R mice compared to I-R mice (+18.3%, p=0.005). At day 30, very small reductions were observed in CTx (5.8%) and Osteocalcin (8.6%) in OVX+R compared to OVX-R without any statistical significance.

Microstructure analysis using microCT

Figure 5 illustrates the resultant changes in bone microarchitecture of both the ovary-intact and ovariectomized distal femur following irradiation. The I+R group experienced a time dependent decrease in trabecular BV/TV that was sizeable and significant by day 30 after the irradiation (Figure 5). t-tests performed within group-cohort (non-radiation – radiation) were significant in the following instances: BV/TV I±R Day 8 cohort = −0.0153, p=0.051; BV/TV I±R Day 30 cohort = 0.0310, p=0.016; Ct.Th I±R Day 8 cohort = −0.0106, p=0.001; and, Ct.Th OVX±R Day 30 cohort = −0.0234, p<0.001.

Comparing group I-R vs. OVX-R, there was a significant difference for Ct.Th (Estimate=0.0244, p=0.047) but not BV/TV. Irradiation had no significant effect on histomorphometric parameters examined in OVX mice, though there was a slight increase in Ct.Th at 30 days.

Using a one-way ANOVA, we compared mice with the same radiation treatment in the I±R groups between days 3, 8 and 30 for both outcomes. We found significant differences between time points for radiated mice only with BV/TV as outcome after multiple comparison adjustments were performed. There was a significant difference between the I +R Day 3 cohort compared to the I−R Day 30 cohort (Estimate=0.0534, p<0.001) and between I+R Day 8 cohort compared to the I−R Day 30 cohort (Estimate=0.0403, p=0.002). There was no significant difference between days 3 and 8.

When comparing cumulative ^{45}Ca vs. BV/TV for the I+R group, the Pearson correlation coefficient was highly significant (Estimate=−0.998, p<0.001) (Figure 6).

Histology / Surface Cellular Activity

Surface activity parameters of static histomorphometry and dynamic histomorphometric parameters are shown in Table 3. In ovary-intact mice, both osteoclasts and osteoblasts seemed to be affected by the local radiation, with a resultant decrease in trabecular perimeter by 30 days. Statistical significance was not observed perhaps due to small number of subjects and large variability in the I+R mice group. As expected, ovariectomy appeared to result in a lower percent of bone perimeter covered by functional osteoblasts and osteoclasts. Delivery of 16Gy local radiation slightly increased osteoclast numbers in the irradiated site, but did not show observable changes in cellular parameters in OVX mice in general.

Dynamic mineralization observed by the Dynamic Histomorphometry and ^{45}Ca excretion

Compared to control, label 1 shows 36.8% reduction in length while 88.7% reduction in label 2 at 17 days later. This represents 51.8% reduction in the rate of change in label length due to radiation during the experimental period (12 to 29 day post radiation). Compared to control, radiation treated mice experienced a modest reduction in MAR (0.00178 μm/day or 16%/day). 35% (3443 DPM/0.2 gm Feces) increase in excretion of ^{45}Ca was observed in same time period with a majority of excretion was observed in between 12 to 20 days post radiation (Figure 4); day 12 increase was 45% while there was only 5.7% increase at day 29.

DISCUSSION/CONCLUSIONS

Although therapeutic radiation and ovariectomy are necessary components for the effective treatment for rectal, endometrial and cervical cancers, the resultant radiation dose and acute-estrogen deficiency contribute to an increased fracture risk and a decreased quality of life [7]. Although co-morbidities have both been shown to affect bone health, little information is available on the dynamics of bone remodeling in response to these influences. This study was designed to gain insight into the longitudinal response of bone mineral remodeling due to cancer therapy in pre- and post-menopausal patients undergoing radiation treatment.

Radiation effect on bone remodeling in ovary-intact vs ovariectomized mice

The purpose of this study was to evaluate the impact of radiation on bone in both an ovary-intact murine model and after acute estrogen deficiency induced by ovariectomy. However, to accomplish this task, the influence of ovariectomy itself on the methods used in this study had to be evaluated to adequately identify changes in the pattern of bone remodeling specific to radiation exposure. The known acute effect of estrogen deficiency to increase bone turnover [28] appears to have been reflected in the significant decrease in cortical thickness in the OVX-R mice compared to the I–R mice at 87 days post ovariectomy (Day 30, Figure 4). Note that the analogous decrease in BV/TV due to ovariectomy only (OVX–R vs. I–R) was not statistically significant.

Interestingly, the effects of radiation varied depending on whether the ovaries were intact or removed, with the main difference manifested as changes in bone microarchitecture occurring within the cancellous or cortical bone. Radiation-induced changes in the ovary-intact groups were primarily within the cancellous bone, while in the ovariectomized animals, they were observed mainly within the cortices. Cortical thickness decreased as a result of ovariectomy, but increased as an effect of radiation in the OVX+R group compared to the OVX–R group. That is, the significant decrease in the cortical thickness, caused by acute estrogen deficiency, was nearly reversed by the remodeling in the OVX+R mice induced after radiation exposure. A radiation-induced increase in the cortical thickness of ovariectomized BALB/c mice is consistent with the findings of Klinck et al. [29], though the radiation exposure examined by this group was a small fraction of the 16Gy employed by the present study (i.e., uCT scans).

Examining the time course of the radiation effect (i.e. increased bone remodeling) in ovary-intact mice revealed an early increase in ^{45}Ca excretion. This is a manifestation of the resultant bone remodeling as evidenced in systemic osteoclastic activity (measured by serum CTx) and osteoblast activity (measured by serum osteocalcin). The time course kinetics of mineral turnover measured by ^{45}Ca excretion is further confirmed with dynamic histomorphometry. As expected, the reduction in mineralization (as measured using MAR and label length) was associated with increased ^{45}Ca excretion. However, the change in MAR reflects accumulated change over the time period post radiation (12–29 days), limiting observation of the real temporal change in bone matrix maturation. Although ^{45}Ca seems to

show rapid change in mineral turnover, it represents whole body turnover, whereas MAR represents local effects of targeted radiation, complementing what is observed in ^{45}Ca assay.

An early increase in bone resorption is consistent with the findings by Willey et al. [30]. However, their study focused on low dose (2 Gy) whole body radiation, results in significant differences compared with local radiation since unexposed skeletal elements may support recovery in the damaged regions. Additionally, our study indicates that this loss may be due to changes in osteoclastic and osteoblastic activities, rather than osteoclast activity alone. This is further supported by the phenomenon observed at the cellular level with decreased osteoclast number, osteoblast surface, and trabecular parameters at day 30. Though, irradiation of ovary-intact animals shows large changes in the number of functional osteoclasts and osteoblastic population; it appeared to have a much smaller effect on OVX mice.

The early increases in bone turnover markers were subsequently followed by significant decreases in BV/TV of the cancellous bone, as measured by microCT-based histomorphometry analysis. As expected, ovariectomy alone appeared to result in a lower percent of bone perimeter covered by functional osteoblasts and osteoclasts. However, delivery of 16Gy did not appear to significantly impact bone. Lack of a significant increase in either ^{45}Ca excretion or markers of bone turnover after radiation in ovariectomized mice may suggest that either a) the changes in bone turnover occurred earlier in ovariectomized mice before markers of bone turnover or calcium excretion were measured as radiation was delivered 57 days post ovariectomy (Schematic figure 1) or b) the decrease in cortical bone occurs independently of ^{45}Ca labeling, which may suggest that ^{45}Ca may preferentially label cancellous bone, possibly due to a higher turnover and larger active bone surface compared to cortical bone. At the cellular level, changes in Ob.S and Oc.N were minimal, with slight increases in Oc.N. A very small reduction in BV/TV was observed (Figure 5). This suggests option (a) as a possible explanation. A lower number of responding cells, possibly due to post-OVX cellular adaptation, may underly the minimal effect of radiation on bone remodeling. In our study, delayed radiation treatment after OVX represents a model similar to the older patient who undergoes radiation treatment long later after their menopause. In the future, an experiment could be designed to assess ovariectomy and radiation consecutively or within a short time difference to assess cumulative effects, modeling the patient who undergoes radiation treatment following menopause.

Biodistribution and Pharmacokinetics of ^{45}Ca

The elevated concentration of ^{45}Ca in the gut tissue on Day 1, rapidly dropping by Day 5, is suggestive of the migration of endogenous ^{45}Ca to feces rather than urine. Spinal ^{45}Ca on Day 1 being nearly equal to the concentration of ^{45}Ca in the gut tissue also indicates a rapid uptake of calcium into this part of the skeleton. The absence of ^{45}Ca in non-skeletal specimens relative to sustained levels of ^{45}Ca in skeletal specimens indicates that the only significant reservoir of ^{45}Ca at the time of irradiation (30 days post-^{45}Ca administration) was in the skeleton. Combined with the steady state of ^{45}Ca excretion attained by 30 days post-^{45}Ca administration, these findings indicate that changes in the concentration of ^{45}Ca in excreta after irradiation of the mice may therefore be a marker for the effects on bone remodeling caused by radiation exposure. Since the majority of excreted ^{45}Ca was via the feces, studies of the time course of ^{45}Ca pharmacodynamics will therefore require that fecal excretion be the focus for long term monitoring via ^{45}Ca assay. Specifically, post-radiation increases in ^{45}Ca excretion would directly reflect increased bone mineral resorption, as confirmed by increased serum osteocalcin concentrations.

Correlation of fecal ^{45}Ca and BV/TV

The significance of increased ^{45}Ca excretion in both mouse models (ovary-intact and ovariectomized) following radiation exposure establishes the benefit of using a biomineral marker for monitoring the impact of therapeutic radiation on bone remodeling. For example, radiation exposure caused a significant early increase in ^{45}Ca excretion and the significant ($p<0.040$) correlation between cumulative ^{45}Ca excretion and decreasing BV/TV (Figure 6) further verified the usefulness of a biomineral marker as a noninvasive, real-time means for predicting and assessing small changes in bone microarchitecture.

Strength and limitations

The early increases of ^{45}Ca excretion, prior to measurable changes in BV/TV, support the use of a calcium tracer for identifying the appropriate time for early intervention to prevent or minimize bone loss. This investigation demonstrates that evaluation of mineral flux with ^{45}Ca in excreta provides a direct, real-time, noninvasive method to monitor treatment-induced changes in bone mineral remodeling that occur rapidly. Importantly, it verifies the efficacy of using a calcium tracer to monitor the early onset and rapid bone turnover associated with therapeutic radiation, thus establishing a clinically relevant murine model for radiation treatment of premenopausal cancer survivors. Nevertheless, there are some limitations. First, small sample sizes within each treatment group of mice may have limited the statistical significance of differences in ^{45}Ca excretion, primarily within the small differences observed in the OVX±R groups. Also, the variation of differences in DPM values is relatively large. We expect that a larger sample size would tend to produce greater statistical significance for the daily differences observed within each group. Second, the experimental period was brief (2 months); a long-term study may be helpful in gaining insight into the inherent course of recovery. Finally, markers of bone turnover were not measured at baseline, prior to ovariectomy. In the future, correlations of ^{45}Ca with bone microstructure and bone mineral content or bone mineral density at a range of time points will be important for developing a predictive model using an isotopic biomarker.

Translational importance

We have recently reported in a study employing quantitative computed tomography (QCT), that patients with ovarian or endometrial cancer experience an accelerated and distinct pattern of trabecular bone loss from systemic chemotherapy vs. local pelvic radiation [31]. The murine models described here simulate the pelvic radiation dosage administered to pre- and post-menopausal women who have endometrial or rectal cancers. The selected experimental radiation dose is considered to be radiobiologically equivalent to the average prescribed clinical dose [21].

Bone damage varies with the dose and the nature of radiation exposure (i.e. local or whole body) [32–35]. The murine models described here demonstrated that ^{45}Ca in an ovary-intact model is sensitive to small changes in skeletal turnover due to local radiation. It is therefore useful for early and long-term monitoring of systemic bone remodeling and is able to show differences related to the etiology of the skeletal damage. Many cancer survivors experience age related or treatment related menopause. Hui et al recently observed that the recovery from skeletal damage may depend on radiation dose with or without ovarian function (i.e., pre- and post-menopausal) [10]. The accurate determination of skeletal damage and ovarian status post cancer treatment may also be essential to select an optimal anti-resorptive pharmacotherapy. This study lays the groundwork to develop a diagnostic marker sensitive enough to design individualized protocols for patients who become osteopenic resulting from cancer treatments. Furthermore, microdose concentrations of ^{41}Ca are known to be highly sensitive to short-term and long-term bone remodeling [18, 19]; since ^{45}Ca can act as

a surrogate marker of ^{41}Ca [20], we expect that ^{41}Ca can be used for analogous investigations in the clinical setting.

In summary, therapeutic radiation affects the pattern of bone mineral remodeling in different ways depending on the ovarian status of the recipient. Use of a real-time, non-invasive ^{45}Ca assay may be useful as a marker to monitor the time course of the bone remodeling response after therapeutic interventions (e.g. radiation exposure) for cancer treatments. Understanding the extent and nature of changes in remodeling and related skeletal damage will be beneficial to optimizing potential interventions during or following cancer therapy.

Acknowledgments

This work was supported by the National Institute of Health grants (1R03AR055333-01A1 and 1K12-HD055887-01). This work was also supported by PHS Cancer Center Support Grant P30 CA77398 and the Joseph E.Wargo cancer research fund from the University of Minnesota. Susanta K Hui is a scholar of the BIRCWH (Building Interdisciplinary Careers in Women's Health) program. The authors acknowledge and thank Luke Arentsen, Kathleen Coghill and Eftu Boru for laboratory assistance. The authors also wish to thank Rajaram Gopalakrishnan, Kim Mansky, and Seymor Levitt for fruitful discussion pertaining to this experiment and manuscript.

References

1. Guise T. Bone loss and fracture risk associated with cancer therapy. The Oncologist. 2006; 11:1121–1131. [PubMed: 17110632]
2. Chen Z, Maricic M, Bassford T, Pettinger M, Ritenbaugh C, Lopez A, Barad D, Gass M, LeBoff M. Fracture risk among breast cancer survivors: Results from the Women's Health Initiative Observational Study. Archives of Internal Medicine. 2005; 165:552. [PubMed: 15767532]
3. Baxter N, Habermann E, Tepper J, Durham S, Virnig B. Risk of pelvic fractures in older women following pelvic irradiation. Am Med Assoc. 2005:2587–2593.
4. Garnero P. Markers of bone turnover for the prediction of fracture risk. Osteoporos Int. 2000; 11(Suppl 6):S55–65. [PubMed: 11193240]
5. Johnell O, Oden A, De Laet C, Garnero P, Delmas P, Kanis J. Biochemical indices of bone turnover and the assessment of fracture probability. Osteoporosis International. 2002; 13:523–526. [PubMed: 12111011]
6. Heaney RP. Is the paradigm shifting? Bone. 2003; 33:457–465. [PubMed: 14555248]
7. Seeman E, Delmas P. Bone quality--the material and structural basis of bone strength and fragility. New England Journal of Medicine. 2006; 354:2250. [PubMed: 16723616]
8. Riis BJ, Hansen MA, Jensen AM, Overgaard K, Christiansen C. Low bone mass and fast rate of bone loss at menopause: Equal risk factors for future fracture: A 15-year follow-up Study. Bone. 1996; 19:9–12. [PubMed: 8830981]
9. Riggs BL, Melton LJ III. Bone Turnover Matters: The Raloxifene Treatment Paradox of Dramatic Decreases in Vertebral Fractures Without Commensurate Increases in Bone Density. Journal of Bone and Mineral Research. 2002; 17:11–14. [PubMed: 11771656]
10. Hui SK, Fairchild GR, Kidder LS, Sharma M, Bhattacharya M, Jackson S, Le C, Yee D. Skeletal Remodeling Following Clinically Relevant Radiation-Induced Bone Damage Treated with Zoledronic Acid. Calcified tissue international. 2011:1–10.
11. Small W Jr, Kachnic L. Postradiotherapy pelvic fractures: cause for concern or opportunity for future research? JAMA. 2005; 294:2635. [PubMed: 16304079]
12. Becker, KL. Principles and practice of endocrinology and metabolism. Lippincott Williams & Wilkins; 2001.
13. Cheong J, Gunaratna N, McCabe G, Jackson G, Weaver C. Bone Seeking Labels as Markers for Bone Turnover: Effect of Dosing Schedule on Labeling Various Bone Sites in Rats. Calcified Tissue International. 2009; 85:444–450. [PubMed: 19763372]

14. Sharma M, Bajzer Z, Hui SK. Development of 41Ca-Based Pharmacokinetic Model for the Study of Bone Remodelling in Humans. Clinical pharmacokinetics. 2011; 50:191–199. [PubMed: 21294596]
15. Välimäki M, Kinnunen K, Volin L, Tähtelä R, Löyttyniemi E, Laitinen K, Mäkelä P, Keto P, Ruutu T. A prospective study of bone loss and turnover after allogeneic bone marrow transplantation: effect of calcium supplementation with or without calcitonin. Bone Marrow Transplantation. 1999; 23:355–361. [PubMed: 10100579]
16. Carlson K, Simonsson B, Ljunghall S. Acute effects of high-dose chemotherapy followed by bone marrow transplantation on serum markers of bone metabolism. Calcified tissue international. 1994; 55:408–411. [PubMed: 7895177]
17. Kang M, Lee W, Oh K, Han J, Song K, Cha B, Lee K, Son H, Kang S, Kim C. The short-term changes of bone mineral metabolism following bone marrow transplantation. Bone. 2000; 26:275–279. [PubMed: 10710001]
18. Denk E, Hillegonds D, Hurrell RF, Vogel J, Fattinger K, Hauselmann HJ, Kraenzlin M, Walczyk T. Evaluation of 41calcium as a new approach to assess changes in bone metabolism: effect of a bisphosphonate intervention in postmenopausal women with low bone mass. J Bone Miner Res. 2007; 22:1518–1525. [PubMed: 17576167]
19. Hui S, Prior J, Gelbart Z, Johnson R, Lentle B, Paul M. A pilot study of the feasibility of long-term human bone balance during perimenopause using a 41Ca tracer. Nuclear Instruments and Methods in Physics Research Section B: Beam Interactions with Materials and Atoms. 2007; 259:796–800.
20. Elmore D, Bhattacaryya MH, Gibson NS. 41Ca as a Long-term Biological Tracer for Bone Resorption. Nucl Instr and Meth. 1990; 52:531–535.
21. Fowler J. Development of radiobiology for oncology-a personal view. Physics in Medicine and Biology. 2006; 51:263.
22. Ma, C. IEEE. 2002. AAPM TG-61 report on kilovoltage X-ray dosimetry: formalisms and applications; p. 2308-2312.
23. Seuntjens, J. IEEE. 2002. AAPM TG-61 report on kilovoltage X-ray dosimetry. II. Calibration procedures and correction factors; p. 2313-2316.
24. Hui SK, Sharma M, Bhattacharyya M. Liquid scintillation based quantitative measurement of dual radioisotopes (^{3}H and ^{45}Ca) in biological samples for bone remodeling studies. Applied Radiation and Isotopes. 2012; 70:63–68. [PubMed: 21900015]
25. Bouxsein M, Boyd S, Christiansen B, Guldberg R, Jepsen K, Müller R. Guidelines for assessment of bone microstructure in rodents using microcomputed tomography. Journal of Bone and Mineral Research. 2010; 25:1468–1486. [PubMed: 20533309]
26. Parfitt AM, Drezner MK, Glorieux FH, Kanis JA, Malluche H, Meunier PJ, Ott SM, Recker RR. Bone histomorphometry: standardization of nomenclature, symbols, and units. Report of the ASBMR Histomorphometry Nomenclature Committee. J Bone Miner Res. 1987; 2:595–610. [PubMed: 3455637]
27. Recker RR, Kimmel DB, Parfitt AM, Davies KM, Keshawarz N, Hinders S. Static and tetracycline-based bone histomorphometric data from 34 normal postmenopausal females. J Bone Miner Res. 1988; 3:133–144. [PubMed: 3213608]
28. Weitzmann MN, Pacifici R. Estrogen deficiency and bone loss: an inflammatory tale. Journal of Clinical Investigation. 2006; 116:1186. [PubMed: 16670759]
29. Klinck J, Campbell GM, Boyd SK. Radiation effects on bone architecture in mice and rats resulting from in vivo micro-computed tomography scanning. Medical Engineering and Physics. 2007
30. Willey J, Lloyd S, Robbins M, Bourland J, Smith-Sielicki H, Bowman L, Norrdin R, Bateman T. Early increase in osteoclast number in mice after whole-body irradiation with 2 Gy X rays. Radiation Research. 2008; 170:388–392. [PubMed: 18763868]
31. Hui Susanta K, Ali Khalil, Yan Zhang, Kathleen Coghill, Chap Le, Kathryn Dusenbery, Jerry Froelich, Douglas Yee, Levi D. Longitudinal assessment of bone loss from diagnostic CT scans in gynecologic cancer patients treated with chemotherapy and radiation. American Journal of Obstetrics & Gynecology. 2010; 203:353.e351–353.e357. [PubMed: 20684943]

32. Cao X, Wu X, Frassica D, Yu B, Pang L, Xian L, Wan M, Lei W, Armour M, Tryggestad E. Irradiation induces bone injury by damaging bone marrow microenvironment for stem cells. Proceedings of the National Academy of Sciences. 2011; 108:1609.

33. Chen H, Lee B, Guo H, Su W, Chiu N. Changes in bone mineral density of lumbar spine after pelvic radiotherapy. Radiotherapy and Oncology. 2002; 62:239–242. [PubMed: 11937252]

34. Overgaard M. Spontaneous Radiation-Induced Rib Fractures in Breast Cancer Patients Treated with Postmastectomy Irradiation A Clinical Radiobiological Analysis of the Influence of Fraction Size and Dose-Response Relationships on Late Bone Damage. Acta Oncologica. 1988; 27:117–122. [PubMed: 3390342]

35. Wientroub S, Weiss J, Catravas G, Reddi A. Influence of whole body irradiation and local shielding on matrix-induced endochondral bone differentiation. Calcified tissue international. 1990; 46:38–45. [PubMed: 2104773]

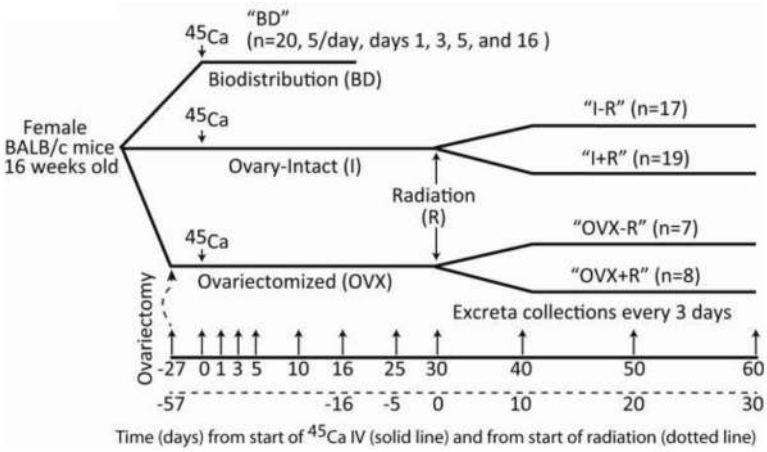

Figure 1.

Schematic of the experimental design. Five groups of skeletally mature BALB/c female mice (16 weeks old) were used for this study. These groups were: 1) Biodistribution (BD); 2) Ovary-intact, non-irradiated (I–R); 3) Ovary-intact, irradiated (I+R); 4) Ovariectomized, non-irradiated (OVX–R); and, 5) Ovariectomized, irradiated (OVX+R). Ovariectomy was performed 27 days prior to ^{45}Ca injection by the vendor (Jackson Laboratory; Bar Harbor, ME) and confirmed by weighing uterii immediately after euthanization.

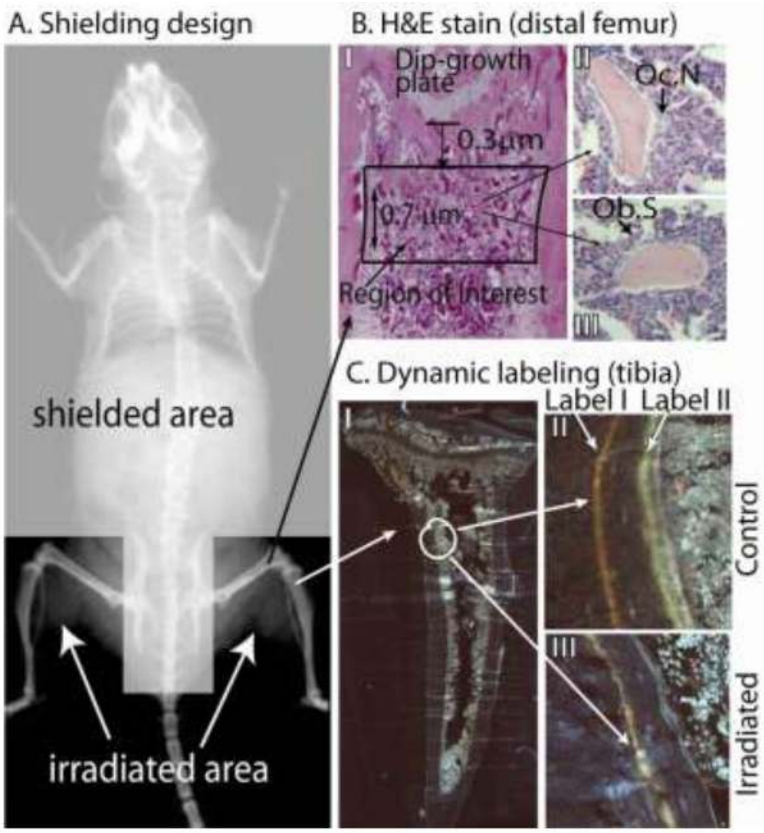

Figure 2.

A. Shielding designed to deliver radiation to the hind limbs while protect the rest of the the animal. A specially designed lead shield (4 mm thickness) was placed over the body cranial to the femur, over the pelvis and caudal vertebrae, targeting the radiation exposure to only the hind limbs. Proper placement of shielding was confirmed using Kodak EDR-2 film placed beneath the animal and acrylic plate. Total dose delivered, including the shielding placement exposure, was 16 Gy. Total dose in the radiation field and under the block was verified using thermo-luminescent dosimeters (TLD). **B.** Hematoxylin and Eosin (H&E) stain (distal femur): (I) Demineralized distal femora vacuum embedded in paraffin were sectioned (5 um) and stained with H&E, then imaged at 100x. (II) the number of osteoclasts (Oc.N), and (III) surface occupied by functional osteoblasts (Ob.S). **C.** Dynamic labeling (proximal tibia). Twelve and twenty nine days post days post radiation, all mice (n=12) received tetracycline and calcein intravenous injections respectively. Mice were euthanized five days later (34d post-radiation). Fixed undemineralized tibiae were vacuum embedded in methyl methacrylate and sectioned at 5 um on an EXAKT system (Oklahoma City, OK) and imaged under UV light with a 40x objective on a Zeiss AxioPlan II (Oberkochen, Germany). Images were captured and stitched together by Image-Pro v7.0 using a Stage-Pro module (Media Cybernetics, Inc., Rockville, MD). A representative figure of collated images of a complete tibia with dual labeling is shown in C (I). A small region of tibia with dual labeling is shown for control mice (II) and for irradiated mice (III).

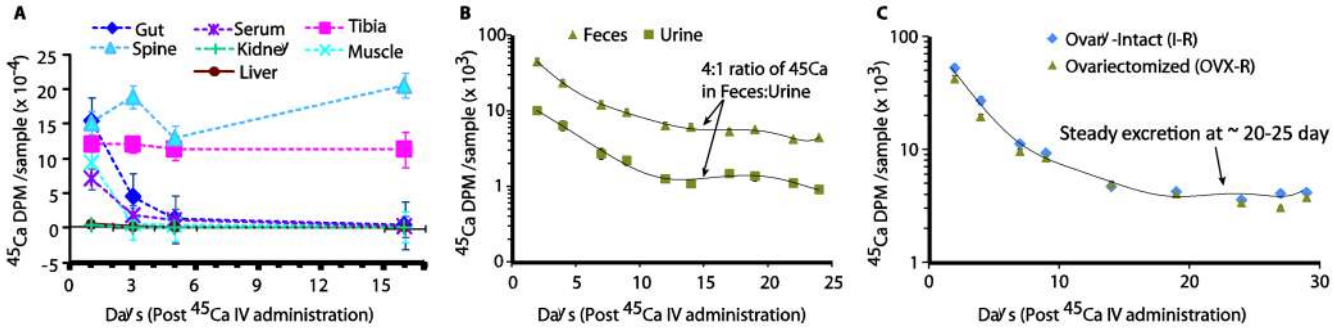

Figure 3.

Biodistribution and pharmacokinetics of ^{45}Ca in various organs, bones and excreta. A. Biodistribution of ^{45}Ca in organs and bones; B: Biodistribution of ^{45}Ca in feces and urine; C. ^{45}Ca pharmacokinetics in feces of different mice groups, I-R and OVX-R. Values are mean ± SE, n=5. To examine isotope biodistribution, ^{45}Ca radioactivity is measured in cleaned and ashed femur, tibia, lumbar vertebrae, liver, kidneys, gut tissue (duodenum to anus, with contents), the quadriceps femoris muscle, urine and feces at days 1, 3, 5, 16. Particulars are detailed in the Methods section.

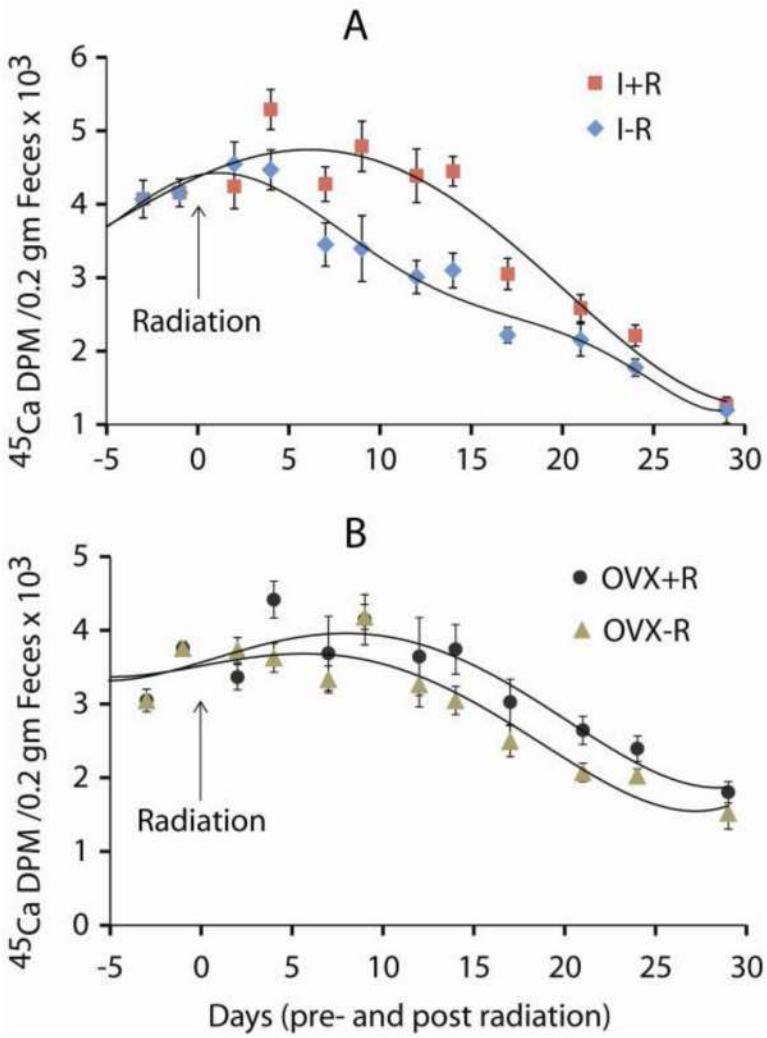

Figure 4.

^{45}Ca excretion curves showing the temporal effect of 16 Gy radiation exposure on the hind limb of ovary-intact mice and ovariectomized (OVX) mice. There was a significant increase in ^{45}Ca excretions from the A). irradiation, ovary-intact group compared to the B). non-irradiated OVX controls ($p<0.001$). Effects of radiation on ^{45}Ca excretion in intact mice were apparent during the first week after treatment emerging transiently (i.e., approximately for two weeks). There appeared to be a smaller effect of radiation on mice ovariectomized 57 days prior.

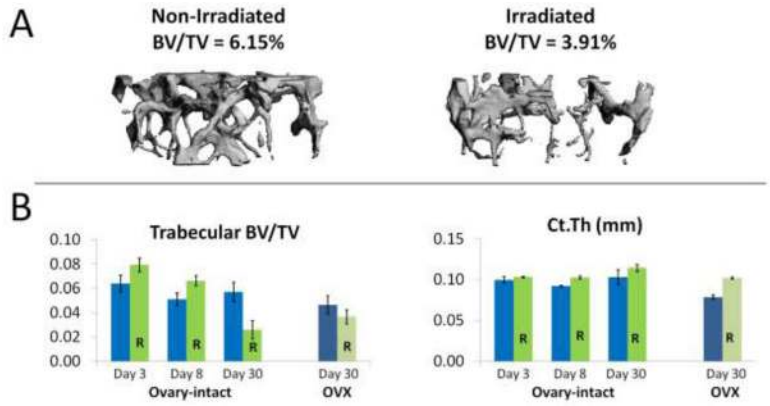

Figure 5.

MicroCT results of the distal femur. A. Representative microCT 3D images of trabecular bone in a non-irradiated (I-R) and an irradiated (I+R) mouse on day 30 after irradiation. The BV/TV of the I+R mouse shown was 36.4% less than that of the I-R mouse shown. B. Histomorphometric parameters for the I±R and OVX±R groups. Histomorphometric parameters shown are: relative cancellous bone volume fraction (BV/TV; %; i.e. the ratio of the segmented bone volume to the total volume of the region of interest) and cortical thickness (Ct.Th, mm). Data are presented as group means ± SEM, n=5–7 per group. Significant differences were observed in the I±R group for BV/TV at day 8 ($p=0.051$) and day 30 ($p=0.016$), but not in the OVX±R group at day 30. A significant difference in Ct.Th was observed in I±R group at day 8 ($p=0.001$), and the OVX±R group at day 30 ($p<0.001$). Time dependent changes in BV/TV were significant (adjusting for multiple comparisons) between the I±R day 3 cohort compared to the I±R day 30 group ($p<0.001$) and between day 8 compared to the day 30 set ($p=0.002$). There was no significant difference between days 3 and 8. Radiation induced reductions in BV/TV were greater in intact mice compared to OVX mice, as is shown by the excreta data (Figure 4).

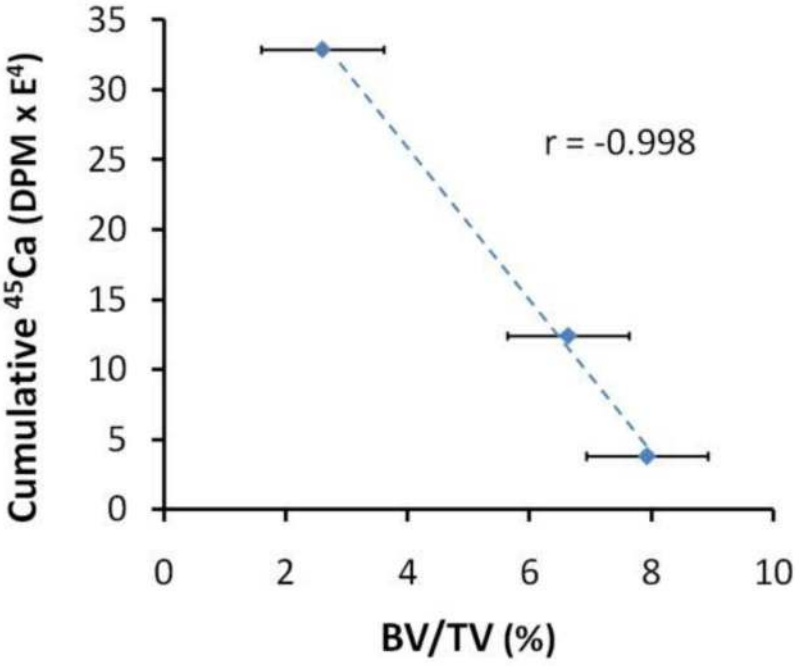

Figure 6.
Correlation of cumulative ^{45}Ca in feces with mean cancellous BV/TV for the I+R group on days 3, 8, and 30 after irradiation ($p<0.001$). Data are presented as means +/− standard error, n=5–7 per group.

Table 1

Group means and standard errors of ^{45}Ca in excreta.

Group	Mean ^{45}Ca in Excreta (DPM/0.2 gm Feces)	Standard Error
Intact − Radiation	3058.8	143.0
Intact + Radiation	3653.7	146.1
Ovariectomized − Radiation	2929.5	113.3
Ovariectomized + Radiation	3285.2	128.7

Table 2

Estimated differences in ^{45}Ca in excreta between irradiated and non-irradiated mice.

Groups	Comparison	Estimate Difference	95% CI	pvalue
Ovary-Intact (I) ± Radiation (R)	I−R − I+R	−889.13	(−1339.74, −438.52)	<0.001
	Slope (I−R) − Slope (I+R)	11.96	(−14.69, 38.60)	0.381
Ovariectomized (OVX) ± Radiation (R)	OVX−R − OVX+R	−211.79	(−815.19, 391.62)	0.493
	Slope (OVX−R) − Slope (OVX+R)	−10.35	(−36.07, 15.37)	0.432

Table 3

Comparative histology data.

	Static Histomorphometry (30 days post radiation)			Dynamic Histomorphometry (12–29 days post radiation)			
	Trabecular Perimeter in μm (±SEM)	**Osteoblast Surface in μm (±SEM)**	**Osteoclast Number**	**12d post-rad (label 1 length in μm (±SEM))**	**29d post-rad (label 2 length in μm (±SEM)**	**Radiation Effect on Flurochrome Incorporation**	**MAR in μm/day (±SEM)**
Intact	1753.7 (435)	5.4 (3)	1.8 (0.5)	2950 (437)	1966 (490)		0.0114 (0.0014)
Intact + Rad	760.8 (227)	2.2 (1)	0.4 (0.2)	1864 (211)	223 (82)		0.0096 (0.0004)
% change	−56.6	−58.7	−77.8	−36.8	−88.7	−51.8	−15.7
OVX	681.1 (395)	0.6 (0.6)	0.8 (0.4)				
OVX+Rad	697.0 (199)	2.2 (1.3)	1.2 (0.4)				